THE JOURNAL OF PHYSICAL CHEMISTRY Letters

Letter

Cite This: J. Phys. Chem. Lett. 2018, 9, 3008−3013

pubs.acs.org/JPCL

Tracer Transport Probes Relaxation and Structure of Attractive and Repulsive Glassy Liquids

Ryan C. Roberts, Ryan Poling-Skutvik, Jeremy C. Palmer,* and Jacinta C. Conrad*

Department of Chemical and Biomolecular Engineering, University of Houston, Houston, Texas 77204-4004, United States

ABSTRACT: Dynamic coupling of small penetrants to slow, cooperative relaxations within crowded cells, supercooled liquids, and polymer matrices has broad consequences for applications ranging from drug delivery to nanocomposite processing. Interactions between the constituents of these and other disordered media alter the cooperative relaxations, but their effect on penetrant dynamics remains incompletely understood. We use molecular dynamics simulations to show that the motions of hard-sphere tracer particles probe differences in local structure and cooperative relaxation processes in attractive and repulsive glassy liquid matrices with equal bulk packing fractions and long-time diffusivities. Coupling of the tracer dynamics to collective relaxations in each matrix affects the shape of tracer trajectories, which are fractal within the repulsive matrix and more compact in the attractive. These results reveal that the structure of relaxations controls penetrant transport and dispersion in cooperatively relaxing systems and provide insight into dynamical heterogeneity within glassy liquids.

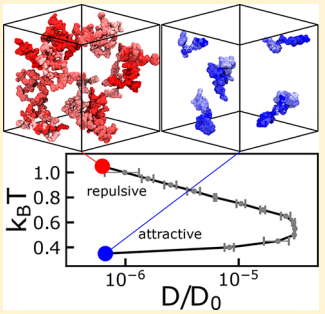

Confined transport within slowly relaxing and structurally disordered matrices governs important processes in physical and biological systems. Controlling the dispersion of particles within polymer matrices, which underpins the functional properties of polymer nanocomposites,[1] requires understanding how the dynamics of nanoparticles in solutions and melts[2,3] relate to those of the polymer matrix.[4] On smaller size scales, the transport of penetrating gas molecules into supercooled or glassy polymer matrices[5,6] governs the efficacy of membrane separation processes.[7,8] Finally, migration and transport in crowded biological systems[9−15] depends on the relaxations of the surrounding crowders. In each process, competition between the relaxations of a disordered matrix and the dynamics of the confined particles can lead to anomalous transport. Although this competition must depend on the structure and nature of the surrounding matrix relaxations, the coupling between tracer transport properties and matrix relaxations remains poorly understood despite its relevance for many physical transport processes.

One of the most intensely studied models of a slowly relaxing system is a dense suspension of colloidal spheres with repulsive interactions. Increasing the sphere volume fraction induces a transition from an ergodic liquid to an arrested glass, driven by entropic crowding.[16,17] Approaching this transition, dynamics become heterogeneous in space and time[18,19] and relaxations occur when particles escape the cages formed by their neighbors, leading to collective string-like rearrangements.[20,21] Weak attractions between particles melt the repulsive glass,[22] whereas stronger interactions lead to the formation of an attractive glass in which dynamics are controlled by caging and interparticle bonds[23−27] and in which collective relaxations are more compact.[28,29] Recent studies on a repulsive colloidal model system reveal that tracers of a critical, relative size can exhibit anomalous logarithmic dynamics, arising from the competition between tracer localization within voids and escape through collective matrix relaxations.[30] Nevertheless, fundamental understanding of how attractive interactions between matrix particles,[31] which are present in all molecular systems, influence tracer transport is critical for advancing most practical applications.

We use event-driven molecular dynamics simulations to show that tracer dynamics within attractive and repulsive glassy matrices with equal packing fractions and long-time diffusivities are remarkably sensitive to differences in matrix structure and dynamics. The tracer dynamics, characterized through the mean-square displacement and the non-Gaussian parameter, depend on tracer size and interactions between matrix particles. Furthermore, they reveal signatures of cage rearrangements in repulsive liquids and, additionally, the competition between bond formation and breaking in attractive liquids. Anomalous, logarithmic tracer dynamics signal a crossover from diffusion within the matrix void space to diffusion coupled to the glassy matrix dynamics and occur on different length scales in repulsive and attractive matrices. As a result of this coupling, the shape of tracer trajectories is different between the two matrices: fractal-like in the repulsive matrix but more compact in the attractive. The sensitivity of tracer dynamics to the confining environment can be exploited to probe subtle differences in the structure of glassy matrices with varying interactions and provides insight into their distinct relaxation processes.

We first examine the dynamics of the two isodiffusive matrices in the absence of tracers. The matrices have identical packing fractions (ϕ = 0.61) and consist of a 50:50 binary AB mixture of species (N = 1372 particles total) with a hard-core diameter ratio σ_{AA}/σ_{BB} 1.2:1 chosen to prevent crystallization.[32]

Received: April 7, 2018
Accepted: May 15, 2018
Published: May 15, 2018

DOI: 10.1021/acs.jpclett.8b01074
J. Phys. Chem. Lett. 2018, 9, 3008−3013

The matrix components have unit mass ($m = 1$) and interact through a short-range square-well potential with depth u_0 and width Δ_{ij} satisfying $\Delta_{ij}/(\sigma_{ij} + \Delta_{ij}) = 0.03$ for each pair type $i,j \in A,B$, where $\sigma_{ij} = \frac{1}{2}(\sigma_{ii} + \sigma_{jj})$. Following convention, we adopt units in which Boltzmann's constant k_B is equal to unity and report length, temperature, and time in terms of σ_{BB}, u_0/k_B, and $\sigma_{BB}(m/u_0)^{1/2}$, respectively. To account for thermal contributions to tracer dynamics, we introduce a normalized time $\tau = tD_0/D_{ref}$, where t is the nominal simulation time, $D_0 = \sigma_{BB}\sqrt{T/m}$ is the thermal diffusivity at T, and D_{ref} is the reference value of D_0 at $T = 1$.

The high-temperature ($T = 1.05$) repulsive glassy matrix (RGM) and low-temperature ($T = 0.35$) attractive glassy matrix (AGM) are ergodic and exhibit nearly equal long-time diffusivities $D_{rep}/D_0 \approx D_{att}/D_0 \approx 6.5 \pm 0.8 \times 10^{-7}$ for species A (Figure 1a), similar to the isodiffusive behavior observed in liquids with density anomalies.[33,34] Both matrices recover these diffusive dynamics on a time scale $\tau \approx 10^4$, indicating that cage escape controls the final relaxation. On intermediate time scales, however, the matrices exhibit different relaxation processes. Particles in the RGM are caged by their neighbors beginning at $\tau \approx 10^0$, with a near-constant normalized mean-squared displacement (MSD, $\langle \Delta\tilde{r}^2 \rangle = \langle \Delta r^2 \rangle / \sigma_{BB}^2$) indicating a localization length of $\sqrt{\langle \Delta\tilde{r}^2 \rangle} = 0.14$. Conversely, the AGM's MSD exhibits only a weak plateau corresponding to a localization length of $\sqrt{\langle \Delta\tilde{r}^2 \rangle} = 0.04$ before increasing as a power law with an exponent less than 1, that is, MSD $\approx \tau^\beta$, $\beta < 1$. Particle motions in the AGM are more localized due to interparticle bonds,[35] so that the extended subdiffusive regime reflects a competition between repulsive caging and attractive bonding.[36] Thus matrix dynamics on intermediate time scales are controlled by caging in the RGM but by both caging and bonding in the AGM.

The different intermediate-time relaxation processes in the AGM and RGM significantly influence the dynamics of confined tracers. We add a small number ($N_t = 10$) of tracer particles with diameter σ_t to the matrices and characterize their equilibrium dynamics through their MSD (Figure 1b–f). The tracers are assigned unit mass and interact with the matrix and other tracer particles through purely repulsive hard-sphere interactions. For small tracers of relative size $\delta = \sigma_t/\sigma_{AB} = 0.20$, the MSDs in both the RGM and AGM exhibit a crossover from ballistic motion on short time scales ($\tau \lesssim 10^0$) to diffusive motion on time scales $\tau > 10^2$ (Figure 1b). The crossover time is nearly identical in the two matrices, indicating that this transition is controlled by hard-sphere steric interactions between tracer and matrix particles. By contrast, the dynamics of larger tracers depend on matrix interactions. In the RGM, the MSD for tracers of size $\delta \geq 0.30$ exhibits an incipient subdiffusive plateau (Figure 1c) whose height decreases and duration increases with increasing tracer size (Figure 1d–f). In the AGM, this subdiffusive plateau is slightly flatter (i.e., the MSD increases less steeply with lag time) and of greater height and longer duration than that in the RGM for tracers of comparable size. Notably, these differences between tracer dynamics are opposite those of the matrix particles (Figure 1a).

The higher intermediate-time plateau in tracer MSDs through the AGM suggests that the tracers explore larger void spaces in the AGM relative to the RGM. To more directly probe the effects of instantaneous matrix structure on tracer dynamics, we simulate tracer dynamics in "frozen" matrix configurations extracted from equilibrium trajectories. Tracer size controls how the structure of the frozen matrix affects their dynamics. The MSDs of small tracers ($\delta = 0.20$) in the frozen and mobile matrices, whether repulsive or attractive, are nearly indistinguishable, indicating that they move easily through the interstitial voids and do not strongly couple to matrix relaxations. Larger tracers, by contrast, exhibit pronounced differences in their dynamics in mobile and immobile matrices that depend on matrix interactions. In the RGM, the tracer MSD in the mobile matrix diverges from that in the immobile matrix before the onset of the plateau (at τ ca. 10^{-1}), indicating that matrix relaxations affect tracer dynamics even on relatively short times. Tracers in the mobile RGM are not fully caged, and their dynamics are subdiffusive over roughly a decade in τ. In the AGM, however, the divergence between tracer MSDs in the mobile and immobile matrices occurs approximately two orders of magnitude later in time (τ ca. 10^1). This result suggests that attractive bonds between matrix particles generate a cage that

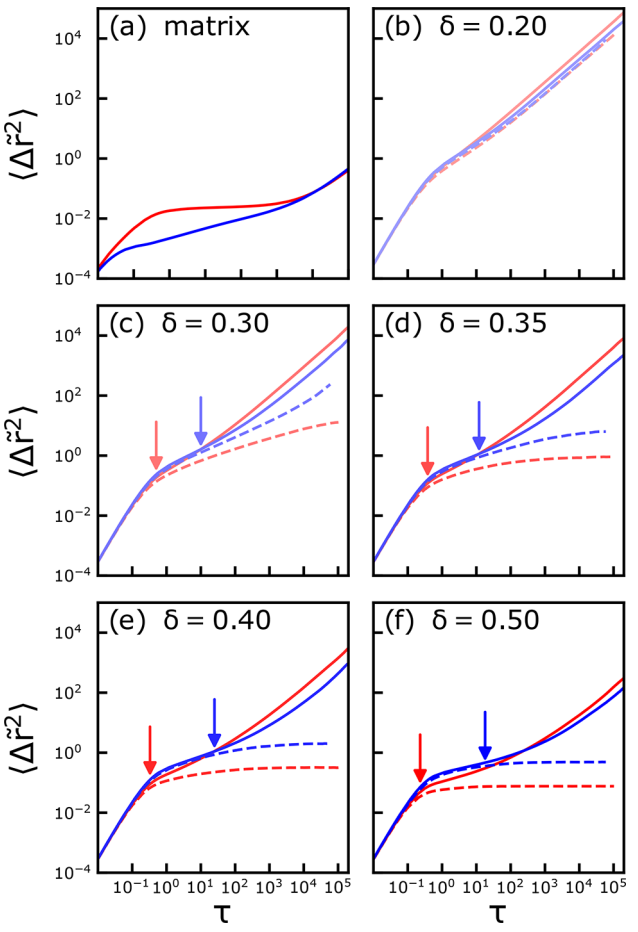

Figure 1. Matrix interactions and tracer size affect tracer dynamics. (a) Mean-square displacement (MSD) $\langle \Delta\tilde{r}^2 \rangle$ for matrix species A normalized to the smaller matrix particle diameter, σ_{BB}, as a function of normalized time scale τ for the RGM (red) and the AGM (blue). Both matrices have an average packing fraction $\phi = 0.61$; the AGM is at a lower temperature $T = 0.35$ and the RGM is at $T = 1.05$. The virial pressures for the two matrices are 1.4 ± 0.1 and 18.9 ± 0.4 u_0/σ_{BB}^3, respectively. (b–f) MSD for tracers of size (b) $\delta = 0.20$, (c) $\delta = 0.30$, (d) $\delta = 0.35$, (e) $\delta = 0.40$, and (f) $\delta = 0.50$ in RGM (red) and AGM (blue) matrices. Solid lines are calculated for matrices that are mobile; dashed lines are calculated for matrices that were immobilized in equilibrium configurations. Arrows indicate the time scale at which the mobile-matrix tracer MSD deviates from that in the immobile matrix.

DOI: 10.1021/acs.jpclett.8b01074
J. Phys. Chem. Lett. 2018, 9, 3008–3013

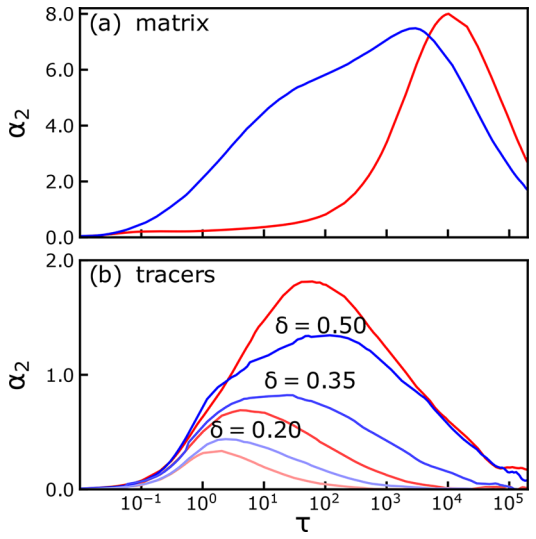

Figure 2. Tracer dynamics are coupled to matrix relaxation processes. (a) Non-Gaussian parameter α_2 as a function of time τ for matrix species A in RGM (red) and AGM (blue). (b) Non-Gaussian parameter α_2 as a function of τ for tracers of size δ = 0.2, 0.35, and 0.5 in RGM (red) and AGM (blue).

relaxes very slowly compared with tracer diffusion, so that tracer particle dynamics are dominated by sampling of arrested cages on short- to intermediate time scales. Because the local environment is more heterogeneous in the AGM (Figure 1), the trajectories of individual tracers therein likewise exhibit a broader distribution of relaxation behaviors. Thus whereas exploration of cages appears to be the dominant mechanism controlling the average tracer dynamics within the AGM, other processes may also play a role. Together, these comparisons indicate that tracer dynamics are affected by both the (instantaneous) structure of glassy matrices and the dynamics of their relaxation processes, leading to tracer dynamics that qualitatively differ from those of the surrounding matrix.

The pronounced difference between the subdiffusive exponents for tracers in the RGM and AGM suggests that local relaxation processes affect tracer diffusion. We characterize the time scales associated with these processes by computing the non-Gaussian parameter $\alpha_2 = 3\langle\Delta\tilde{r}^4\rangle/5\langle\Delta\tilde{r}^2\rangle^2 - 1$ as a function of lag time. The shape and relaxation times identified by α_2 differ between the RGM and AGM (Figure 2a). The α_2 for the RGM exhibits the classic behavior expected for a supercooled colloidal liquid,[18] attaining a local maximum at τ ca. 10^4, the time scale at which the matrix particle dynamics become diffusive and cages are disrupted (Figure 1a). The α_2 for the AGM, however, first exhibits a shoulder at τ ca. 10 and then reaches a maximum near $\tau \lesssim 10^4$. The broad maximum in α_2 for the AGM is consistent with the idea that rearrangements in attractive glassy liquids occur over a broader range of time scales[28] and, hence, likely, length scales than those of a repulsive glassy liquid.

The α_2 values for the tracers are smaller than those obtained for their corresponding matrices (Figure 2b) and exhibit a maximum at a particular time scale τ shorter than the time scale in the matrix. The time scale corresponding to maximum non-Gaussianity increases with increasing tracer size. For small tracers of size δ = 0.20, α_2 attains a maximum near τ ca. 1 in both the RGM and AGM. The greater height and width of the maximum of the tracer α_2 in the AGM indicate that the tracer

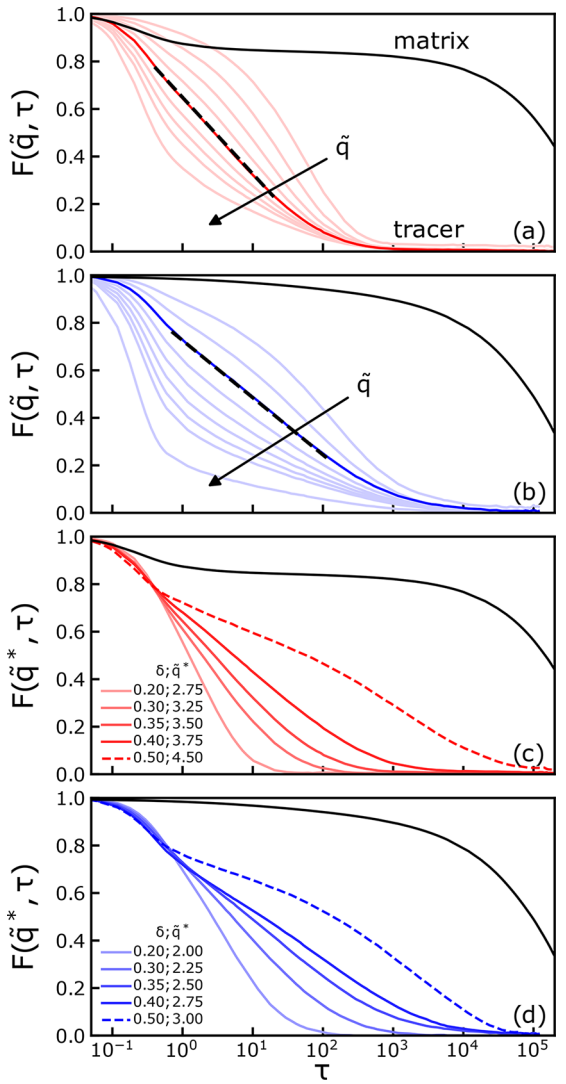

Figure 3. Tracers in RGMs and AGMs exhibit anomalous transport. (a,b) Collective intermediate scattering function $F(\tilde{q},\tau)$ for tracers of size δ = 0.35 within the (a) RGM and (b) AGM for reduced scattering vectors $\tilde{q} = q\sigma_{BB}$ = 1.5, 2.0, 2.5, 3.0, 3.5, 4.0, 4.5, 5.0, and 6.0. The arrow indicates increasing $\tilde{q}$. $\tilde{q}^*$ indicates the wavevector at which logarithmic decay appears; $\tilde{q}^*$ = 3.5 in the RGM and $\tilde{q}^*$ = 2.5 in the AGM, as indicated by the black dashed lines in panels a and b. (c,d) $F(\tilde{q}^*,\tau)$ for tracers of varying size δ in the (c) RGM and (d) AGM, shown at the wavevector $\tilde{q}^*$ at which the decay is logarithmic (as indicated). $F(\tilde{q},\tau)$ for the corresponding A matrix particles is shown in black at the wavevector corresponding to the first peak in the matrix static structure factor $S(\tilde{q})$ ($\tilde{q}$ = 6.7).

dynamics in the AGM are slightly more heterogeneous than in the RGM. When δ = 0.35, the shapes of the tracer α_2 in the RGM and AGM become dissimilar. In the RGM, the maximum in α_2 increases in height and width with increasing tracer size; it remains approximately Gaussian in shape but shifts to larger τ ($\sim 10^2$ at δ = 0.50). By contrast, α_2 in the AGM becomes increasingly broad as δ increases. For all tracer sizes, α_2 increases rapidly up to $\tau \approx 10^0$ and then increases more slowly to reach a maximum that shifts to greater τ as δ is increased; this evolution reflects broad coupling to cage relaxations occurring on these time scales. Thus the α_2 measurements reveal heterogeneous tracer dynamics on distinct time scales that depend on both tracer size and matrix interactions, with

DOI: 10.1021/acs.jpclett.8b01074
J. Phys. Chem. Lett. 2018, 9, 3008−3013

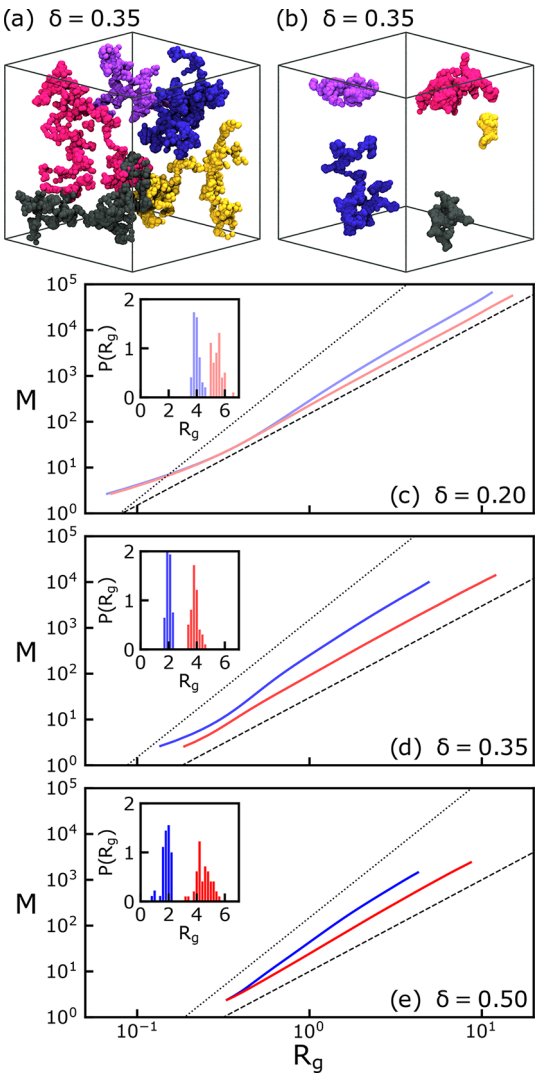

Figure 4. Tracers in RGMs and AGMs explore space differently. (a,b) Representative trajectories of tracers of size $\delta = 0.35$ in the (a) RGM and (b) AGM. (c–e) Trajectory mass M as a function of trajectory radius of gyration R_g for tracers of size (c) $\delta = 0.2$, (d) $\delta = 0.35$, and (e) $\delta = 0.5$ in RGM and AGM. Dashed and dotted lines in panels c–e correspond to power laws of 2 and 3, respectively. Insets in panels c–e: Probability distribution functions for trajectory R_g at 5000 coarse-grained time steps.

increasing coupling to matrix dynamics as the tracer size is increased.

To gain insight into the length scales over which tracer dynamics are coupled to matrix relaxations, we examine the collective intermediate scattering functions (ISFs, $F(\tilde{q},\tau)$). From the ISF, it is clear that tracer dynamics depend on tracer size, matrix interactions, and length scale $2\pi/\tilde{q}$, where $\tilde{q} = q\sigma_{BB}$ is the normalized scattering wave vector (Figure 3). We first scrutinize the dynamics of tracers of size $\delta = 0.35$ as a function of $\tilde{q}$ in the different matrices. At low $\tilde{q}$, the ISF of a tracer in the RGM decays nearly exponentially (Figure 3a). At $\tilde{q} \approx 3.5$, however, $F(\tilde{q},\tau)$ exhibits a logarithmic decay over two orders of magnitude in time for nearly its entire relaxation process. The onset of the logarithmic dynamics occurs at approximately the time scale at which the matrix relaxes and is close to the time scale ($\tau \approx 1$) at which the tracer α_2 attains a maximum; these comparisons suggest that these logarithmic dynamics arise when the tracers become transiently localized. Similar logarithmic decay is observed for tracers of size $\delta \leq 0.40$ in the RGM and in the AGM (Figure 3b) but not for tracers with size ratio $\delta = 0.50$.

Logarithmic relaxations in glassy systems are usually interpreted as a consequence of competing arrest mechanisms.[35,37−41] Because the matrix relaxations are not logarithmic, the logarithmic dynamics of the tracers do not reflect competing arrest mechanisms in the matrix but instead indicate a crossover between local processes controlling their dynamics. Similar crossovers have been proposed for other confined transport systems. Partially pinned particles exhibit logarithmic behavior, for example, as they undergo a crossover from localized to glassy dynamics.[42,43] Closer to our work, the extended logarithmic dynamics observed in ref 30 were attributed to two competing processes, transient localization, and matrix crowding. Hence we posit that the length scale of the logarithmic dynamics reflects the length scale on which tracer dynamics become coupled to the slow relaxations of the matrix. In contrast with the study of ref 30, which examined tracer diffusion in liquids and in glasses and also observed extended logarithmic relaxations, we examine only liquids, as the use of isodiffusive matrices allows us to remove effects arising from the long-time dynamics. Thus in our study the self- and collective ISFs do not decouple because both matrices are ergodic on long time scales.

The value of $\tilde{q}$ where logarithmic decay appears, $\tilde{q}^*$, depends on tracer size and matrix interactions.[30] In both matrices, $\tilde{q}^*$ increases with tracer size (Figure 3b,c), indicating that relaxation processes compete on smaller length scales. Furthermore, for a fixed tracer size the wavevector of the logarithmic dynamics is smaller in the AGM than in the RGM. Two mechanisms may explain the decrease in relaxation length scales with increasing tracer size: Larger tracers more frequently contact surrounding matrix particles and less frequently encounter fluctuations in the matrix large enough for the tracer to enter. Both mechanisms reduce the mobility of tracers and, because the matrix relaxations do not change with tracer size, lead to a decrease in the length scale corresponding to logarithmic decay. Indeed, tracers of size $\delta = 0.5$ exhibit the multistep relaxations characteristic of deeply supercooled colloids,[36] but no logarithmic decay is observed at any $\tilde{q}$. Our data also indicate that tracers in the AGM couple to relaxations on larger length scales than those in the RGM, attributable to the slower dynamics of the AGM on intermediate time scales ($10^0 \lesssim \tau \lesssim 10^4$, Figure 1a). The fact that the tracer dynamics are logarithmic over different length scales in the RGM and AGM suggests that the tracers couple to the different mesoscale relaxation processes of the two matrices.

In glassy colloidal liquids, the morphology of mesoscale relaxations depends on matrix interactions; relaxing regions in attractive glasses are reported to be more compact than those in repulsive glasses.[28,29] To assess whether the shape of relaxing regions affects the ability of tracers to explore space, we directly visualize the tracer trajectories, coarse-graining over a time scale, $\tau_{cg,\delta}$, that for a given δ removes cage exploration processes and the effects of thermal diffusion. For tracers of size $\delta = 0.2$, we choose $\tau_{cg,0.2} = 0.05$ for both matrices. For larger tracers, we use $\tau_{cg,\delta} = \tau_{cg,0.2}(\tau_{cage,\delta}/\tau_{cage,0.2})$ to remove the effects of cage exploration, where $\tau_{cage,\delta}$ is chosen to satisfy $\langle \Delta\tilde{r}^2(\tau_{cage,\delta})\rangle/\sigma_t^2 = 1.0$. Representative trajectories for tracers of size $\delta = 0.35$ have distinct morphologies in the two matrices (Figure 4a,b). Tracer trajectories are tenuous and fractal-like in the RGM but more

DOI: 10.1021/acs.jpclett.8b01074
J. Phys. Chem. Lett. 2018, 9, 3008−3013

compact in the AGM. We characterize this difference in shape by examining the tracer trajectory mass, M, calculated as the number of boxes of size $\sqrt{\langle \Delta \tilde{r}^2(\tau_{cg,\delta}) \rangle}$ (the square-root of the tracer MSD at the coarse-grained time scale, $\tau_{cg,\delta}$) needed to cover the trajectory, as a function of the trajectory radius of gyration R_g.[44,45] The mass of tracer trajectories in the RGM scales as a power law with R_g, that is, $M \approx R_g^{d_f}$, and the resultant long-time fractal dimension $d_f \approx 2.0$ is approximately independent of the tracer size. This fractal scaling of the tracer trajectories corresponds to free diffusion and is expected for both matrices, which are ergodic on long time scales. For tracer trajectories in the AGM, however, M is larger than that in the RGM at a given R_g; likewise, the instantaneous slope is larger and does not approach the expected terminal scaling with R_g of 2.0 on accessible time scales. Thus tracer trajectories in the AGM are more compact than those in the RGM on similar length and time scales.

Our simulations reveal that the spatiotemporally heterogeneous dynamics in glassy liquids of varying matrix particle interactions alter the dynamics of hard-sphere tracers. The tracers couple to relaxation processes in repulsive and attractive matrices on distinct time and length scales. As a result, tracers exhibit trajectories of different shape in the two matrices, indicating that matrix interactions alter the ability of tracers to explore space within a slowly relaxing matrix. Because dispersing particles within slowly relaxing matrices with varying interactions appear in settings ranging from the crowded cytoplasm inside cells to natural soils in the environment to artificial fiber nanocomposites and membranes, these results provide insight into the coupling between particle transport and matrix dynamics across a wide range of scientifically and technologically relevant processes.

AUTHOR INFORMATION

Corresponding Authors

*J.C.P.: E-mail: jcpalmer@uh.edu.
*J.C.C.: E-mail: jcconrad@uh.edu.

ORCID

Ryan Poling-Skutvik: 0000-0002-1614-1647
Jeremy C. Palmer: 0000-0003-0856-4743
Jacinta C. Conrad: 0000-0001-6084-4772

Notes

The authors declare no competing financial interest.

ACKNOWLEDGMENTS

We thank the Welch Foundation (E-1869 and E-1882) and the National Science Foundation (CBET-1705968) for support.

REFERENCES

(1) Kumar, S. K.; Benicewicz, B. C.; Vaia, R. A.; Winey, K. I. 50th Anniversary Perspective: Are Polymer Nanocomposites Practical for Applications? *Macromolecules* **2017**, *50*, 714−731.
(2) Grabowski, C. A.; Mukhopadhyay, A. Size Effect of Nanoparticle Diffusion in a Polymer Melt. *Macromolecules* **2014**, *47*, 7238−7242.
(3) Poling-Skutvik, R.; Krishnamoorti, R.; Conrad, J. C. Size-Dependent Dynamics of Nanoparticles in Unentangled Polyelectrolyte Solutions. *ACS Macro Lett.* **2015**, *4*, 1169−1173.
(4) Cai, L.-H.; Panyukov, S.; Rubinstein, M. Mobility of Nonsticky Nanoparticles in Polymer Liquids. *Macromolecules* **2011**, *44*, 7853−7863.
(5) Zhang, R.; Schweizer, K. S. Correlated Matrix-Fluctuation-Mediated Activated Transport of Dilute Penetrants in Glass-Forming Liquids and Suspensions. *J. Chem. Phys.* **2017**, *146*, 194906.
(6) Zhang, K.; Meng, D.; Muller-Plathe, F.; Kumar, S. K. Coarse-Grained Molecular Dynamics Simulation of Activated Penetrant Transport in Glassy Polymers. *Soft Matter* **2018**, *14*, 440−447.
(7) Geise, G. M.; Lee, H.-S.; Miller, D. J.; Freeman, B. D.; McGrath, J. E.; Paul, D. R. Water Purification by Membranes: The Role of Polymer Science. *J. Polym. Sci., Part B: Polym. Phys.* **2010**, *48*, 1685−1718.
(8) Sanders, D. F.; Smith, Z. P.; Guo, R.; Robeson, L. M.; McGrath, J. E.; Paul, D. R.; Freeman, B. D. Energy-Efficient Polymeric Gas Separation Membranes for a Sustainable Future: A Review. *Polymer* **2013**, *54*, 4729−4761.
(9) Lee, S.-H.; Bardunias, P.; Su, N.-Y.; Yang, R.-L. Behavioral Response of Termites to Tunnel Surface Irregularity. *Behav. Processes* **2008**, *78*, 397−400.
(10) Roosen-Runge, F.; Hennig, M.; Zhang, F.; Jacobs, R. M. J.; Sztucki, M.; Schober, H.; Seydel, T.; Schreiber, F. Protein Self-Diffusion in Crowded Solutions. *Proc. Natl. Acad. Sci. U. S. A.* **2011**, *108*, 11815−11820.
(11) Di Rienzo, C.; Piazza, V.; Gratton, E.; Beltram, F.; Cardarelli, F. Probing Short-Range Protein Brownian Motion in the Cytoplasm of Living Cells. *Nat. Commun.* **2014**, *5*, 5891.
(12) Angelini, T. E.; Hannezo, E.; Trepat, X.; Marquez, M.; Fredberg, J. J.; Weitz, D. A. Glass-Like Dynamics of Collective Cell Migration. *Proc. Natl. Acad. Sci. U. S. A.* **2011**, *108*, 4714−4719.
(13) Schötz, E.-M.; Lanio, M.; Talbot, J. A.; Manning, M. L. Glassy Dynamics in Three-Dimensional Embryonic Tissues. *J. R. Soc., Interface* **2013**, *10*, 20130726.
(14) Garcia, S.; Hannezo, E.; Elgeti, J.; Joanny, J.-F.; Silberzan, P.; Gov, N. S. Physics of Active Jamming During Collective Cellular Motion in a Monolayer. *Proc. Natl. Acad. Sci. U. S. A.* **2015**, *112*, 15314−15319.
(15) Gravish, N.; Gold, G.; Zangwill, A.; Goodisman, M. A. D.; Goldman, D. I. Glass-Like Dynamics in Confined and Congested Ant Traffic. *Soft Matter* **2015**, *11*, 6552−6561.
(16) Stevenson, J. D.; Schmalian, J.; Wolynes, P. G. The Shapes of Cooperatively Rearranging Regions in Glass-Forming Liquids. *Nat. Phys.* **2006**, *2*, 268−274.
(17) Garrahan, J. P.; Chandler, D. Geometrical Explanation and Scaling of Dynamical Heterogeneities in Glass Forming Systems. *Phys. Rev. Lett.* **2002**, *89*, 035704.
(18) Kob, W.; Donati, C.; Plimpton, S. J.; Poole, P. H.; Glotzer, S. C. Dynamical Heterogeneities in a Supercooled Lennard-Jones Liquid. *Phys. Rev. Lett.* **1997**, *79*, 2827−2830.
(19) Pastore, R.; Pesce, G.; Sasso, A.; Pica Ciamarra, M. Cage Size and Jump Precursors in Glass-Forming Liquids: Experiment and Simulations. *J. Phys. Chem. Lett.* **2017**, *8*, 1562−1568.
(20) Donati, C.; Douglas, J. F.; Kob, W.; Plimpton, S. J.; Poole, P. H.; Glotzer, S. C. Stringlike Cooperative Motion in a Supercooled Liquid. *Phys. Rev. Lett.* **1998**, *80*, 2338−2341.
(21) Weeks, E. R.; Crocker, J. C.; Levitt, A. C.; Schofield, A.; Weitz, D. A. Three-Dimensional Direct Imaging of Structural Relaxation Near the Colloidal Glass Transition. *Science* **2000**, *287*, 627−631.
(22) Foffi, G.; Dawson, K. A.; Buldyrev, S. V.; Sciortino, F.; Zaccarelli, E.; Tartaglia, P. Evidence for an Unusual Dynamical-Arrest Scenario in Short-Ranged Colloidal Systems. *Phys. Rev. E: Stat. Phys., Plasmas, Fluids, Relat. Interdiscip. Top.* **2002**, *65*, 050802R.
(23) Reichman, D. R.; Rabani, E.; Geissler, P. L. Comparison of Dynamical Heterogeneity in Hard-Sphere and Attractive Glass Formers. *J. Phys. Chem. B* **2005**, *109*, 14654−14658.
(24) Pham, K. N.; Petekidis, G.; Vlassopoulos, D.; Egelhaaf, S. U.; Poon, W. C. K.; Pusey, P. N. Yielding Behavior of Repulsion- and Attraction-Dominated Colloidal Glasses. *J. Rheol.* **2008**, *52*, 649−676.
(25) Zaccarelli, E.; Poon, W. C. K. Colloidal Glasses and Gels: the Interplay of Bonding and Caging. *Proc. Natl. Acad. Sci. U. S. A.* **2009**, *106*, 15203−15208.

DOI: 10.1021/acs.jpclett.8b01074
J. Phys. Chem. Lett. 2018, 9, 3008−3013

(26) Koumakis, N.; Petekidis, G. Two Step Yielding in Attractive Colloids: Transition from Gels to Attractive Glasses. *Soft Matter* **2011**, *7*, 2456−2470.
(27) van de Laar, T.; Higler, R.; Schroën, K.; Sprakel, J. Discontinuous Nature of the Repulsive-to-Attractive Colloidal Glass Transition. *Sci. Rep.* **2016**, *6*, 22725.
(28) Zhang, Z.; Yunker, P. J.; Habdas, P.; Yodh, A. G. Cooperative Rearrangement Regions and Dynamical Heterogeneities in Colloidal Glasses with Attractive Versus Repulsive Interactions. *Phys. Rev. Lett.* **2011**, *107*, 208303.
(29) Brown, Z.; Iwanicki, M. J.; Gratale, M. D.; Ma, X.; Yodh, A. G.; Habdas, P. Correlated Rearrangements of Disordered Colloidal Suspensions in the Vicinity of the Reentrant Glass Transition. *Europhys. Lett.* **2016**, *115*, 68003.
(30) Sentjabrskaja, T.; Zaccarelli, E.; De Michele, C.; Sciortino, F.; Tartaglia, P.; Voigtmann, T.; Egelhaaf, S. U.; Laurati, M. Anomalous Dynamics of Intruders in a Crowded Environment of Mobile Obstacles. *Nat. Commun.* **2016**, *7*, 11133.
(31) Parmar, A. D. S.; Sastry, S. Kinetic and Thermodynamic Fragilities of Square Well Fluids with Tunable Barriers to Bond Breaking. *J. Phys. Chem. B* **2015**, *119*, 11243−11252.
(32) Zaccarelli, E.; Foffi, G.; Sciortino, F.; Tartaglia, P. Activated Bond-Breaking Processes Preempt the Observation of a Sharp Glass-Glass Transition in Dense Short-Ranged Attractive Colloids. *Phys. Rev. Lett.* **2003**, *91*, 108301.
(33) Coslovich, D.; Ikeda, A. Cluster and Reentrant Anomalies of Nearly Gaussian Core Particles. *Soft Matter* **2013**, *9*, 6786−6795.
(34) Bertolazzo, A. A.; Barbosa, M. C. Phase Diagram and Thermodynamic and Dynamic Anomalies in a Pure Repulsive Model. *Phys. A* **2014**, *404*, 150−157.
(35) Dawson, K.; Foffi, G.; Fuchs, M.; Götze, W.; Sciortino, F.; Sperl, M.; Tartaglia, P.; Voigtmann, T.; Zaccarelli, E. Higher-Order Glass-Transition Singularities in Colloidal Systems with Attractive Interactions. *Phys. Rev. E: Stat. Phys., Plasmas, Fluids, Relat. Interdiscip. Top.* **2000**, *63*, 011401.
(36) Zaccarelli, E.; Foffi, G.; Dawson, K. A.; Buldyrev, S. V.; Sciortino, F.; Tartaglia, P. Confirmation of Anomalous Dynamical Arrest in Attractive Colloids: A Molecular Dynamics Study. *Phys. Rev. E: Stat. Phys., Plasmas, Fluids, Relat. Interdiscip. Top.* **2002**, *66*, 041402.
(37) Sciortino, F.; Tartaglia, P.; Zaccarelli, E. Evidence of a Higher-Order Singularity in Dense Short-Ranged Attractive Colloids. *Phys. Rev. Lett.* **2003**, *91*, 268301.
(38) Moreno, A. J.; Colmenero, J. Logarithmic Relaxation in a Kinetically Constrained Model. *J. Chem. Phys.* **2006**, *125*, 016101.
(39) Moreno, A. J.; Colmenero, J. Relaxation Scenarios in a Mixture of Large and Small Spheres: Dependence on the Size Disparity. *J. Chem. Phys.* **2006**, *125*, 164507.
(40) Mayer, C.; Sciortino, F.; Likos, C. N.; Tartaglia, P.; Löwen, H.; Zaccarelli, E. Multiple Glass Transitions in Star Polymer Mixtures: Insights from Theory and Simulations. *Macromolecules* **2009**, *42*, 423−434.
(41) Gnan, N.; Das, G.; Sperl, M.; Sciortino, F.; Zaccarelli, E. Multiple Glass Singularities and Isodynamics in a Core-Softened Model for Glass-Forming Systems. *Phys. Rev. Lett.* **2014**, *113*, 258302.
(42) Kim, K.; Miyazaki, K.; Saito, S. Slow Dynamics in Random Media: Crossover from Glass to Localization Transition. *Europhys. Lett.* **2009**, *88*, 36002.
(43) Kurzidim, J.; Coslovich, D.; Kahl, G. Dynamic Arrest of Colloids in Porous Environments: Disentangling Crowding and Confinement. *J. Phys.: Condens. Matter* **2011**, *23*, 234122.
(44) Zierenberg, J.; Fricke, N.; Marenz, M.; Spitzner, F. P.; Blavatska, V.; Janke, W. Percolation Thresholds and Fractal Dimensions for Square and Cubic Lattices with Long-Range Correlated Defects. *Phys. Rev. E: Stat. Phys., Plasmas, Fluids, Relat. Interdiscip. Top.* **2017**, *96*, 062125.
(45) Saberi, A. A. Fractal Structure of a Three-Dimensional Brownian Motion on an Attractive Plane. *Phys. Rev. E: Stat., Nonlinear, Soft Matter Phys.* **2011**, *84*, 021113.

DOI: 10.1021/acs.jpclett.8b01074
J. Phys. Chem. Lett. 2018, 9, 3008−3013